ALKAAD

ALKAAD Photonics

Teaching and Operation Manual

Open Frame Helium Neon Laser

Compiled by
Akanksha Goyal

and
Mukul Goyal

Contents

1   Introduction

The first ever operated laser was an optically pumped solid state laser. This laser has been discovered by Theodore Maiman in 1960 [1]. The active material was the element 24, chromium, which was embedded into a transparent host crystal. The host crystal is a corundum crystal also known as aluminium oxide (Al_2O_3). The chromium dopant replaces some aluminium atoms thus changing the optical properties of the crystal. The so doped crystal shows a red colour and is also known as ruby.

^{1}H																	^{2}He
^{3}Li	^{4}Be											^{5}B	^{6}C	^{7}N	^{8}O	^{9}F	^{10}Ne
^{11}Na	^{12}Mg											^{13}Al	^{14}Si	^{15}P	^{16}S	^{17}Cl	^{18}Ar
^{19}K	^{20}Ca	^{21}Sc	^{22}Ti	^{23}V	^{24}Cr	^{25}Mn	^{26}Fe	^{27}Co	^{28}Ni	^{29}Cu	^{30}Zn	^{31}Ga	^{32}Ge	^{33}As	^{34}Se	^{35}Br	^{36}Kr
^{37}Rb	^{38}Sr	^{39}Y	^{40}Zr	^{41}Nb	^{42}Mo	^{43}Tc	^{44}Ru	^{45}Rh	^{46}Pd	^{47}Ag	^{48}Cd	^{49}In	^{50}Sn	^{51}Sb	^{52}Te	^{53}I	^{54}Xe
^{55}Cs	^{56}Ba	57..71	^{72}Hf	^{73}Ta	^{74}W	^{75}Re	^{76}Os	^{77}Ir	^{78}Pt	^{79}Au	^{80}Hg	^{81}Tl	^{82}Pb	^{83}Bi	^{84}Po	^{85}At	^{86}Rn
^{87}Fr	^{88}Ra	89..103	^{104}Rf	^{105}Db	^{106}Sg	^{107}Bh	^{108}Hs	^{109}Mt	^{110}Ds	^{111}Rg	^{112}Cn	^{113}Uut	^{114}Fl	^{115}Uup	^{116}Lv	^{117}Uus	^{119}Uuo

	^{57}La	^{58}Ce	^{59}Pr	^{60}Nd	^{61}Pm	^{62}Sm	^{63}Eu	^{64}Gd	^{65}Tb	^{66}Dy	^{67}Ho	^{68}Er	^{69}Tm	^{70}Yb	^{71}Lu
	^{89}Ac	^{90}Th	^{91}Pa	^{92}U	^{93}Np	^{94}Pu	^{95}Am	^{96}Cm	^{97}Bk	^{98}Cf	^{99}Es	^{100}Fm	^{101}Md	^{102}No	^{103}Lr

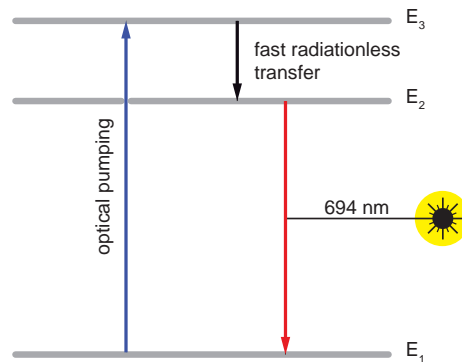Figure 1: Periodic table of the elements

Figure 2: Simplified three level system of the ruby laser

The ruby laser boosted a tremendous research effort and initiated a hunt for other more promising laser materials. One of the major drawbacks of the ruby laser was the fact that it could only operate in pulsed mode. This is due to its three level laser system as shown in figure 1. By excitation with suitable light chromium ions of the ground state (E_1) are excited and consequently populate the excited state (E_3).

From here the only way back to the ground state is via the E_2 energy level. In a first step the excited Cr ions are transferring a fraction of their energy to the lattice of the host crystal and are assembling in the energy level E_2. The transfer from $E_3 \to E_2$ is very fast and takes place in a few picoseconds.

Note: Population inversion is hard to achieve in a three energy level system like the ruby laser.

However the energy level E_2 is a so called metastable state. This means that the Cr ions are trapped in this state, since an optical transition to the ground state is forbidden due to the selection rules of quantum mechanics for electromagnetic transitions. Nature is not strictly merciless and a forbidden transition still has a certain probability and can be considered as a weak optical transition. Nevertheless the Cr ions will remain approximately five micro seconds in the E_2 state, which is fairly long for optical transitions, before they reach the ground state again.

$$N_2 - N_1 = \frac{2\pi n^2 \nu^2}{c^2} \tag{1}$$

We learned that a laser process can only start, if the so called Schawlow-Townes [2] oscillation condition (1) is fulfilled. The equation shows a simplified version of it. In this equation n stands for the index of refraction, ν for the laser frequency and c for the speed of light, N_2 is the population density of energy level E_2 and N_1 accordingly. Only if $N_2 - N_1$ is greater zero the equation yields useful results. In other words the population density of state E_2 must be greater than that of state E_1. This situation is also termed as population inversion [3].
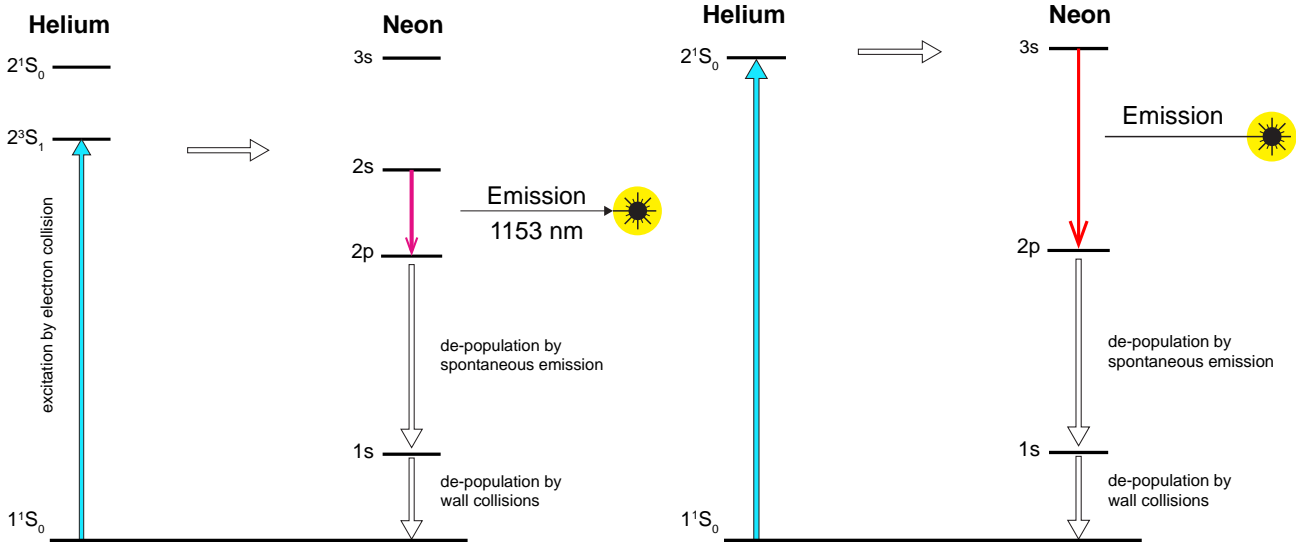
Figure 3: Laser cycle first operated by Ali Javan [2]

Figure 4: Visible laser emission as operated by White and Rigden in 1962 [4]

Such an inversion is hard to reach since N_1 is the population of the ground state, which is always populated. Only under "hard pumping" most Cr ions will be transferred to E_2. We have just five microseconds time to almost empty the ground state before the delayed transfer from E_2 starts to populate the ground state again.

This is one of the reasons that a ruby laser in general emits pulsed laser radiation. On the search for a more suitable laser material the element 60 (neodymium) turned out to be a good candidate. Laser operation of neodymium was first demonstrated by J. E. Geusic et al. at Bell Laboratories in 1964 [5].

However, in the same year of the invention of the ruby laser, Ali Javan in December of 1960 discovered the first gas laser operating in continuous wave mode (cw) [3].

The outstanding property of such a HeNe laser lies in the fact that the laser process takes place inside a sort of a four level energy system (see figures 3 and 4). This and the extreme purity and coherence of the laser emission made this laser to an indispensable tool for a great variety of applications.

Although the diode laser took over a great range of applications, the HeNe laser is still used in laser gyroscopes in all air craft for GPS independent navigation, and for highly precise laser metrological applications like industrial laser interferometer for the calibration of CNC machines. Furthermore this laser system is an integral part of the lectures in photonics worldwide, since it is based on atomic energy levels and teaches about the operation of a laser cavity in an comprehensible manner.

From figure 4 we can conclude that the laser oscillation condition (1) is already fulfilled once the excitation takes place. In this system the population inversion is created between the energy levels $2s$ and $2p$ (Javan) or $3s$ and $2p$. Because the $2p$ energy level is far above the ground state, its population is zero. So even a single excited $2s$ or $3s$ Neon atom provides a population inversion.

2   Helium Neon Laser

2.1   Energy level system

When quantum mechanics was developed, it had to be validated and verified that it was able to describe nature. For the examination only atoms like hydrogen (H), helium (He) and neon (Ne) were simple enough to be started with. As a result of this the spectroscopic data of H, He, and Ne have been known very precisely. The mathematical complexity dramatically increases with atoms having multiple electrons and considering all possible interaction in many particle systems was and is too tedious.

Based on this, Javan et. al. first tried the He Ne system. It was already known by this time that the 2^1S_0 and the 2^3S_0 states of helium are so called metastable. This means that from here no optical transitions are possible to the ground state. It means also that all transitions from higher lying states of helium will be trapped in these two states. Excitation by an electrical discharge is a broadband excitation that fills all possible exited states of helium, but all transitions are terminating in these two metastable states 2^1S_0 and 2^3S_0 which in turn get densely populated.

And this is the trick of the Helium Neon laser which is commonly not discussed in text books. Many times students raise the question, ".... why not excite the Neon directly by discharge? Why do we need the Helium?"

Assuming we are only using neon atoms and exciting them by a gas discharge we would populate almost all states of it. Thus we are not able to create a population inversion which is required for laser operation or in other words we cannot fulfil the Schawlow-Townes oscillation condition [5].

If into the discharge tube containing neon we add helium, even 10 times more than neon, we selectively populate the $3s$ and $2s$ states of the neon atoms via the 2^1S_0 and 2^3S_0 states of helium since this is the most efficient way for the helium atoms to reach ground state.

The combination of the trick of using helium to obtain a population inversion in neon and applying the spectroscopic data makes the invention of A. Javan even more admirable. A fascinating source to learn how this invention happened can be found by following the link mentioned at [2] of the list of references.
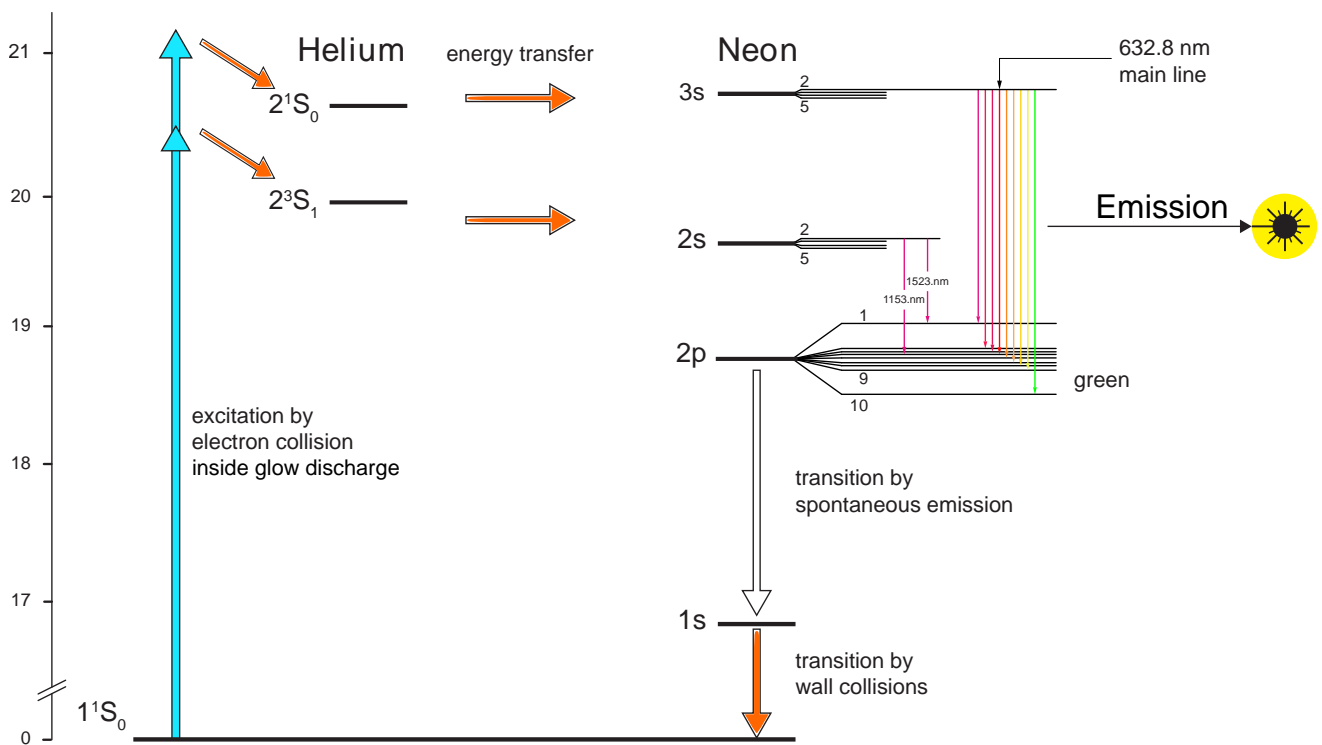

Figure 5: Simplified energy level diagram of the HeNe laser system
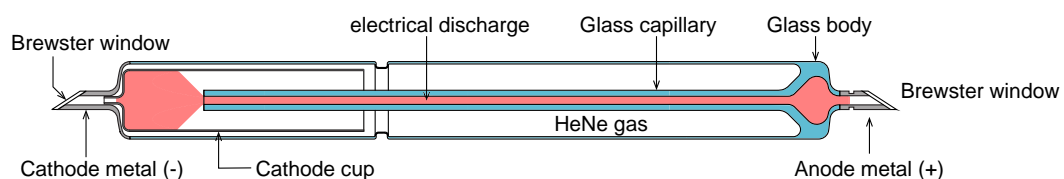
2.2   Principle of operation

Figure 6: Cut through a HeNe laser tube with Brewster widows on both sides

Each laser cycle can be described as a virtual flow of excited "particles". One nice method to do it is termed rate equation model [8]. The idea is to identify and remove as far as possible "bottle necks" in the process. Even without applying mathematics it can be recognised that the last step of the laser cycle of neon, the emptying of the $1s$ state to the ground state, is such a bottle neck.

The only way to do it is to let the excited Neon atoms run against a wall. This is why the helium neon laser requires the glass capillary. The $1s$ bottle neck is also the reason why the helium neon laser is limited to 50-100 mW output power and never could become a high power laser. The task for the engineers was to find an optimum of a small capillary diameter to best match the mode volume of the surrounding optical cavity.

An example of such an optimised laser tube is shown in figure 6 and is the same one which is used in the experiments. Two Brewster windows are attached to the end of the tube. By adding two well aligned and coated mirrors an open frame HeNe resonator is formed. The complete experimental HeNe laser is described in the following chapter.
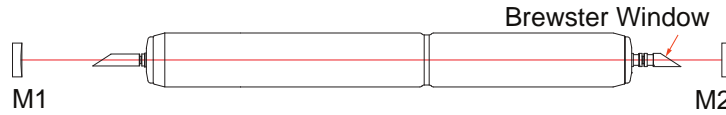
Figure 7: Principle of open frame HeNe laser
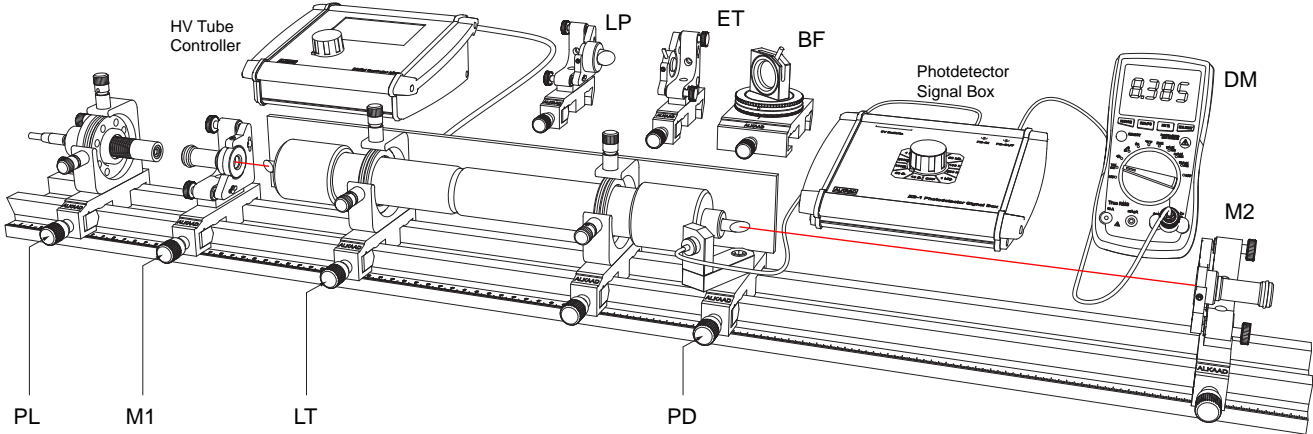
3   Experimental Set-up

Figure 8: Helium Neon Experimental Laser Setup

The figure above shows the setup using a precise optical rail and the modules for line selection as well as single mode operation. The following chapters describe the individual components and modules in detail.

3.1   Description of the components

3.1.1   Optical rail

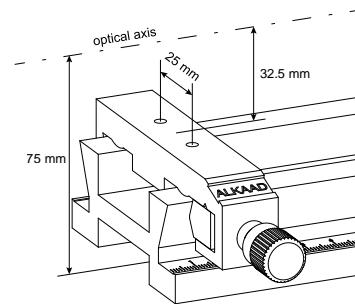Figure 9: Platinum-Iridium meter bar [9]

Figure 10: Rail system

The ALKAAD rail and carrier system (figure 10) provides a high degree of integral structural stiffness and accuracy. The idea for this structure is based on the form of the reference meter of Paris and was further optimised for daily laboratory use. The optical height of the optical axis is chosen to be 75 mm above the table surface. The optical height of 32.5 mm above the carrier surface is compatible with many other systems like those from MEOS, LUHS, MICOS. OWIS and LD Didactic. Consequently a high degree of system compatibility is achieved.

3.1.2   Pre-adjustment laser PL

When Javan set up the first continuously operating laser, he had no other laser to align the mirror of the cavity. At that time, this task was accomplished by a specialist experienced with interferometer sand auto collimating telescopes. Nowadays we make use on a green laser pointer which is mounted into a precise five axes adjustment holder.

By means of four adjustment screws the laser beam can be aligned orthogonally in XY direction and tilted in two orthogonal angles.
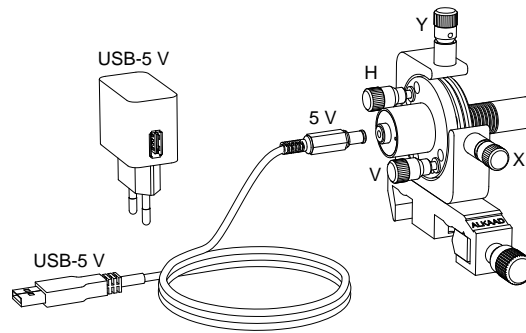
Figure 11: Pilot laser module (PL)

3.1.3 Laser mirror adjustment holders "left" and "right"
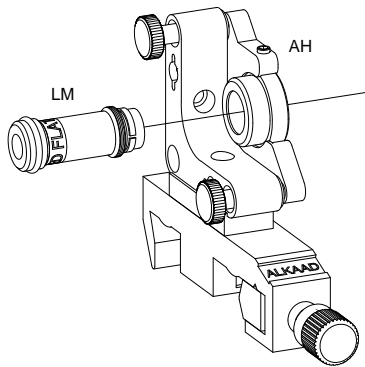

Figure 12: Laser mirror adjustment holder "left" with mirror M1
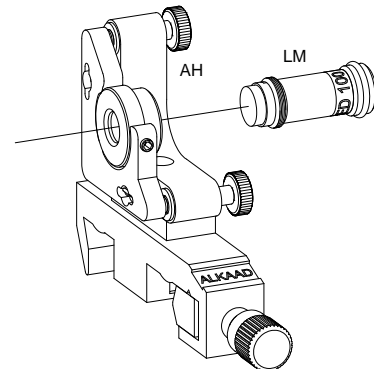

Figure 13: Laser mirror adjustment holder "right" with mirror M2

The adjustment holders (AH) comprise two high precision fine pitch screws. The upper screw is used to tilt the moveable plate vertically and the lower one to tilt it horizontally.

The mounting plate provides a M16 mount into which the laser mirror holders (LM) are screwed. The mirror is pressed against a mechanical reference plane inside the M16 mount in such a way that the mirror is always aligned perfectly when removed and screwed in again.

The adjustment holder is either mounted to the carrier in the "left" operating mode to hold the left cavity mirror M1 or in the "right" mode to hold the right cavity mirror M2.

Due to the symmetry of the adjustment holder (AH) it can also be changed from the "right" to the "left" mode and vice versa if required.
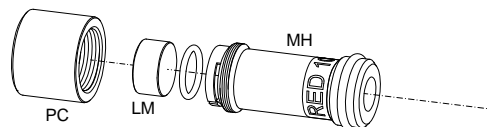
3.1.4 Set of laser mirrors

Figure 14: Mounted laser mirror

The set-up comprises two sets of mirrors each mounted separately as shown in figure 14. Each mirror has the standard diameter of 12.7 mm (1/2 inch) and a thickness of 6.35 mm (1/4 inch). The laser mirror (LM) is mounted into the holder (MH) and kept in position by two spring loaded flaps. A soft O-ring provides a soft seat of the mirror inside the holder (MH) especially when screwed into the adjustment holder.

The mirrors are of supreme quality, coated by ion beam sputtering (IBS) yielding the highest degree of reflectivity and lowest scatter losses achievable until date. A cap (PC) protects the sensitive mirrors when not in use. Each mirror is labelled and the meaning of the markings is given in the following table:

Marking and labelling of the mirrors:

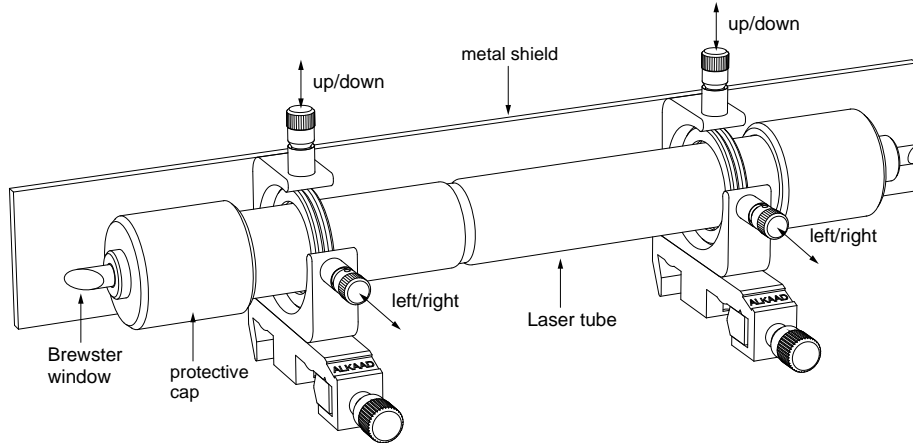| Mark	Coating	Label	Geometry
RED	HR 580...720 nm	RED FLAT	flat mirror
NIR	HR 1050...1250 nm	RED 750	ROC 750 mm
HR	R > 99.98 %	RED 1000	ROC 1000 mm
ROC	radius of curvature	NIR FLAT	flat mirror
		NIR 750	ROC 750 mm

3.1.5 The HeNe laser tube (LT)

Figure 15: HeNe laser tube module (LT)

The laser tube is mounted into two XY adjustment holders. The tube can be aligned parallel to the X and Y direction as well as slightly turned about an axis perpendicular to the optical axis which is necessary to align the capillary with respect to the optical axis of the laser cavity which may deviate from the axis of the optical rail (e.g. could be set by beam walking). It can be turned about its long axis to set the angle of polarisation of the Brewster windows, e.g. to make it coincide with that of the birefringent tuner (BFT).

A metal shield carries on its rear the ballast resistor required for a stable high voltage discharge. Both the anode and cathode are insulated so there is no electrical hazard. The Brewster windows are protected by soft silicon caps when the tube is not in operation.

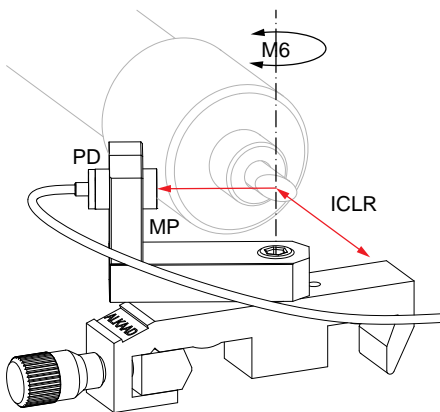### 3.1.6 Si PIN photodetector module (PD)

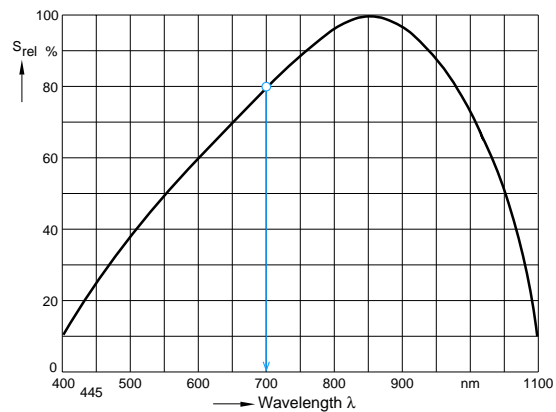
Figure 16: Photodetector module

Figure 17: Sensitivity curve of the BPX61 photodiode

A Si PIN photodiode is integrated into a small housing and accommodated inside an aperture (MP) attached to the swivel arm to pick up the light reflected from the Brewster window. Connected to the ZB1 box by a BNC cable, it can either detect low light intensities using high resistances or fast signals up to 1 GHz using low resistances. Signals transporting the beat frequency of the laser modes are in the 100 MHz range, thus fast.

Parameter	Symbol	Value	Unit
Current rise, fall time at $R_L = 50\Omega; V_R = 5V; \lambda = 850\ nm$ and $Ip = 800\mu A$	t_r, t_f	20	ns
Forward voltage $I_F = 100mA, E = 0$	V_F	1.3	V
Capacitance at $V_R = 0, f = 1MHz$	C_0	72	pF
Wavelength of max. sensitivity	λ_{Smax}	850	nm
Spectral sensitivity S 10% of S_{max}	λ	1100	nm
Dimensions of radiant sensitive area	L x W	7	mm^2
Dark current, $V_R = 10V$	IR	≤ 30	nA
Spectral sensitivity, $\lambda = 850\ nm$	$S(\lambda)$	0.62	A/W

Table 1: Basic parameters of Si PIN photodiode BPX61

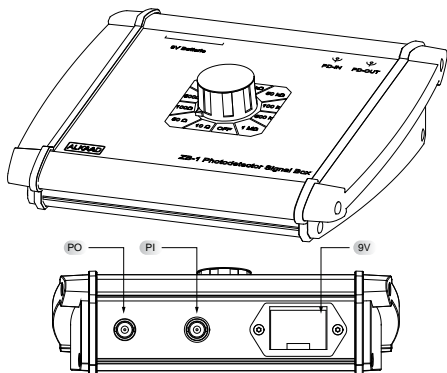### 3.1.7 Photodetector Signal Box ZB1

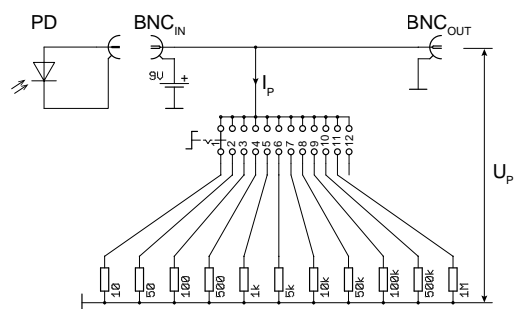
Figure 18: Signal Box ZB1

Figure 19: Signal box schematic

The signal box contains a resistor network and a replaceable 9 V battery. It can work with all kind of photodiodes provided they are connected to the BNC input (PD-IN) as shown in the schematic of figure 19. At the output (PD-OUT) of the signal box a signal is present which is given by the following equation:

$$I_P = \frac{U_p}{R_L}$$

I_P is the photo current created by illuminating the photodiode with light. U_p is the voltage drop across the selected load resistor R_L. To convert the measured voltage into a respective optical power we have to make use of the spectral sensitivity $S(\lambda)$ [A/W] which depends on the wavelength of the incident light according to figure 17. The detected optical power P_{opt} in W can be given as:

$$P_{opt} = \frac{I_p}{S(\lambda)}$$

Assuming a wavelength of 700 nm we take the value of S_{rel} from figure 17 as 0.8 and the spectral sensitivity from the last row of table 1 as 0.62 A/W, so the value of $S(\lambda = 700\ nm)$ is $0.62\ A/W \cdot 0.8 = 0.496\ A/W$. If we measure a voltage U_m of 5 V with a selected load resistance R_L of 1 kΩ, the optical power will be

$$P_{opt} = \frac{I_p}{S(\lambda)} = \frac{U_p}{R_L \cdot S(\lambda)} = \frac{5\ V}{1000\ \frac{V}{A} \cdot 0.496\ \frac{A}{W}} = 10\ mW$$

It must be noted that the measured power is correct only if the entire light beam hits the detector.

Based on the selected load resistor the sensitivity will be high for higher resistances, but the rise and fall time will be longer, because the diode capacitance with the load resistor forms a RC low pass filter. For fast signals a low resistance should be used, however the sensitivity will be lower.

3.1.8 Birefringent tuner (BFT)

A detailed description of the property and function of a double refractive tuning element can be found in [10] or [11].

The double refractive or birefringent plate (P) is mounted in a dual rotational stage. For the intra-cavity operation the birefringent plate (P) needs to be aligned in such a way that the laser beam hits the plate under the Brewster angle to minimize the reflection losses. This can be accomplished by turning the rotary plate (B).

In addition the birefringent plate can be rotated around its optical axis by tilting the lever (L).

By rotating the plate (P), its optical retardation δ, the path difference between ordinary and extraordinary ray, is changed. Only if the retardation after two passes through the plate is a multiple integer of the wavelength, the plane of polarisation remains unchanged and there are no additional losses at the Brewster windows.

3.1.9   Littrow prism tuner (LPT)

Another way to select different lines of a laser is to use a Littrow prism. A detailed description of tuning a HeNe Laser with a Littrow prism is given by [11].

In this experiment we are using such a module to tune the helium neon laser. The Littrow prism is made from fused silica which is the required substrate for ion beam sputtering (IBS) coating.

The spectral range of the IBS coating covers 580...720 nm with a reflectivity ¿99.98 %. The prism is mounted into a precise adjustment holder where it can be smoothly tilted in vertical or horizontal direction.
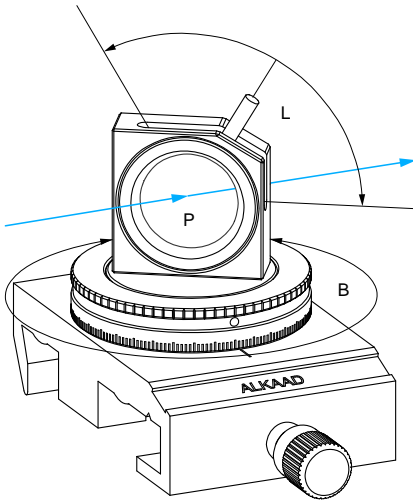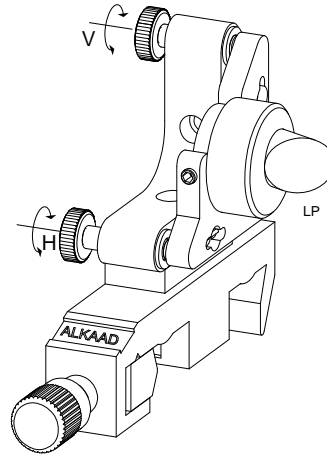

Figure 20: Optional birefringent tuner

Figure 21: Optional Littrow prism tuner
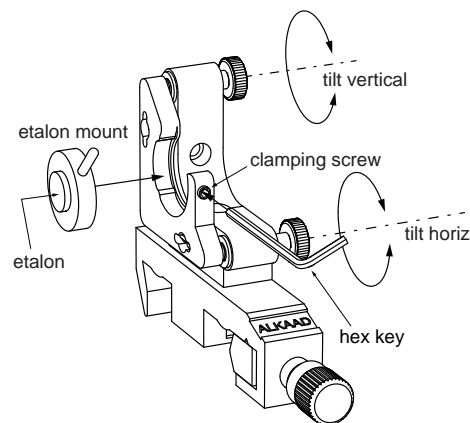
3.1.10   Single Mode Etalon

Figure 22: Single mode etalon

To force the laser to operate in only one longitudinal mode a so called etalon is used. It consists of a quartz cylinder with its end faces precisely ground parallel within a few arc seconds. The length is designed such that the convolution of its wavelength dependent transmission function with the HeNe cavity wavelength dependent resonator quality function favours only one single mode.

The etalon is mounted into a holder which is inserted into the adjustment holder. A provided hexagon key is used to fix the etalon mount. Two precise fine pitch screws allow the sensitive tilt of the etalon which is required to tune it inside the cavity to different orders of the etalon. Further details or the properties of such an etalon can be found in [11] and in the chapter 4.6.1 of this manual.

3.1.11 High voltage controller

Figure 23: Digital controller MK1

Figure 24: Start-up screen

The high voltage controller is a novel and safe combination of high voltage constant current source and micro processor control. The HeNe laser tube is connected via a special high voltage BNC connector to the rear of the controller. The precision five turn potentiometer sets the discharge current in a range from 4.5 to 7 mA.

When the device is connected to an external 12 V supply, the controller starts displaying the start-up screen as shown in Fig. 24 for approximately 3.5 seconds. After that the user is requested to enter a four digit pin code for authorization.
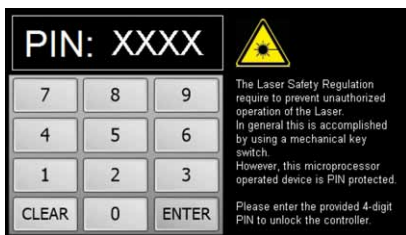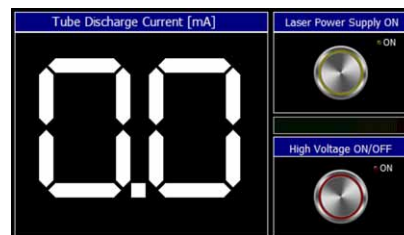

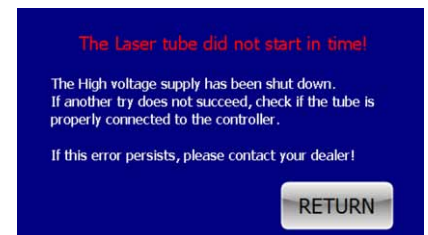Figure 25: Entry screen

Figure 26: Main screen

Figure 27: Laser tube warning screen

Laser safety

According to laser safety regulations [12] unauthorized operation must be prevented. So the first interactive screen, see Fig. 25, requires the log in to the device. In general this is accomplished by using a mechanical key switch, but this microprocessor operated device provides a better protection by requesting the entry of a PIN.

After entering the proper key the next screen is displayed and the system is ready for operation.

Main screen

When pressing the start button, the controller applies a start voltage of up to 8 kV to ignite a glow discharge in the tube. If the glow discharge does not start within 2 seconds and the set constant current is not reached, the controller switches off its high voltage module.

Once successfully started, the current through the discharge tube can be set by turning the knob of the 5 turn potentiometer. The controller measures and displays the real tube current, see Fig. 26.

Failure screen

If the tube does not start within 2 seconds then the failure screen shows up, see Fig. 27. It is advising the user to connect the tube to the controller if that has not been done before.

4 Experimental set-up and Measurements

It is the aim to setup and align the HeNe laser and perform a variety of measurement tasks.

1. Basic alignment
2. Optical stability criteria
3. Gaussian beams
4. Excitation spectrum

5. Wavelength selection with Littrow prism

6. Wavelength selection with BFT

7. Single mode operation with etalon

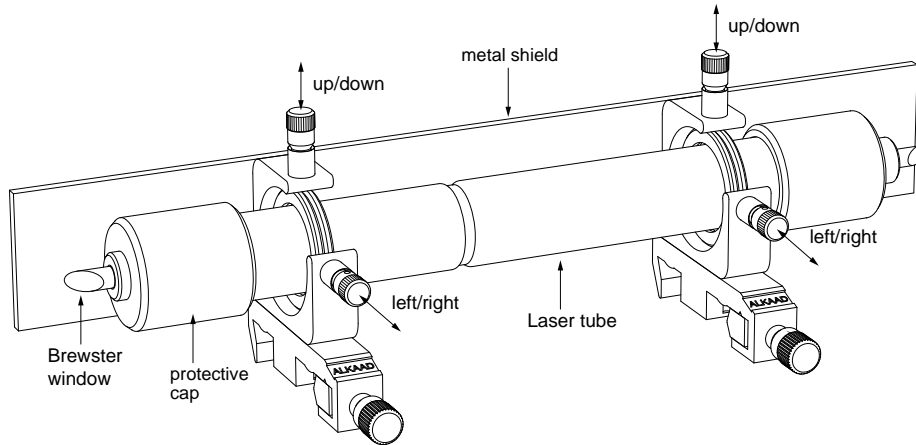8. Longitudinal modes

4.1   Basic alignment

Figure 28: HeNe laser tube

The laser tube is visually centred to the mechanical axes of the adjustment holder. This forms the reference for all other components and defines the direction of the capillary.

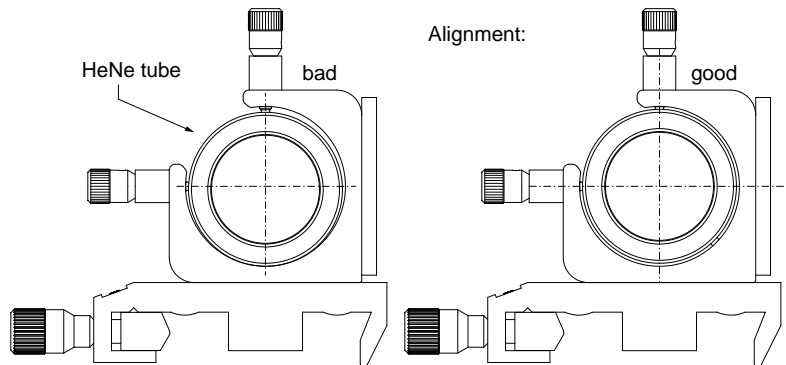Once the system is operating the adjustment screws can be used to optimise the laser cavity.

4.1.1   Centering the tube

Figure 29: Centric tube alignment
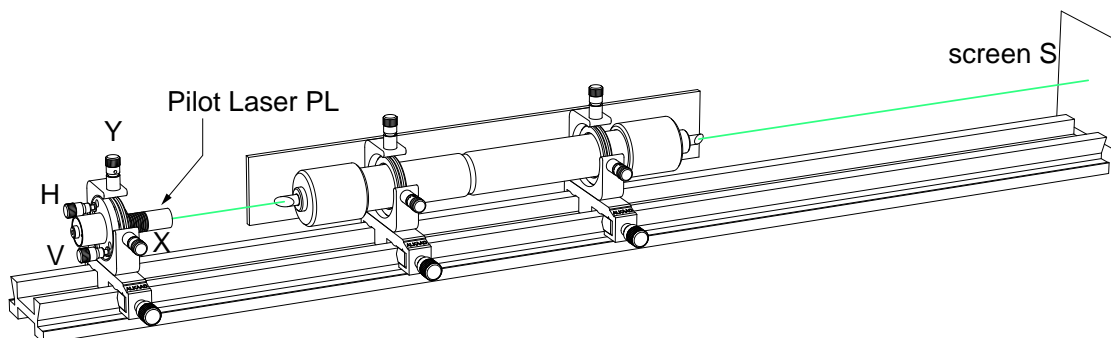
4.1.2   Pilot Laser alignment

Figure 30: Align the pilot laser

Place the prepared laser tube onto the rail. Align the pilot laser in such a way that the green laser passes through the capillary of the HeNe tube unhindered. Check this with a sheet of white paper or check the image on the wall of the lab.
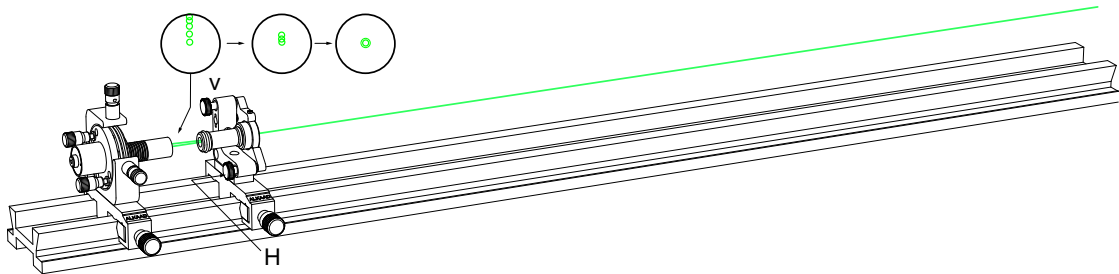
4.1.3 Align the left mirror

Figure 31: Alignment of the left mirror M1

Now the green laser beam is the reference for the capillary as well as for the rest of the components.

Insert the flat mirror and align its back reflex with the green laser outlet so that the beam is multiply reflected. Then bring the manifold reflexes all to coincide as shown in the figure on the left.
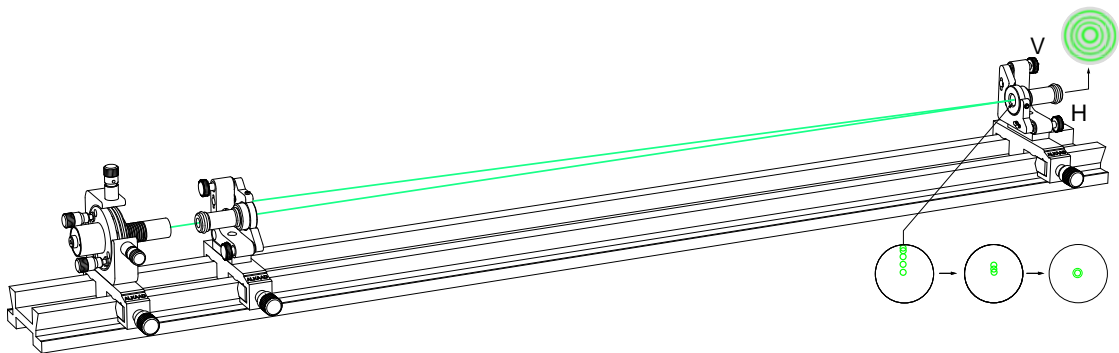
4.1.4 Align the right mirror

Figure 32: Alignment of the right mirror M2

It is good practise to start with the right mirror (M2) having a radius of curvatures of 750 mm.

Also centre the reflected beam to the green spot of the flat mirror.

Image the green beams again on a piece of white paper or watch it on the lab wall. When properly aligned, the cavity becomes resonant for the green light, starts flickering, and shows concentric Fabry Perot rings.
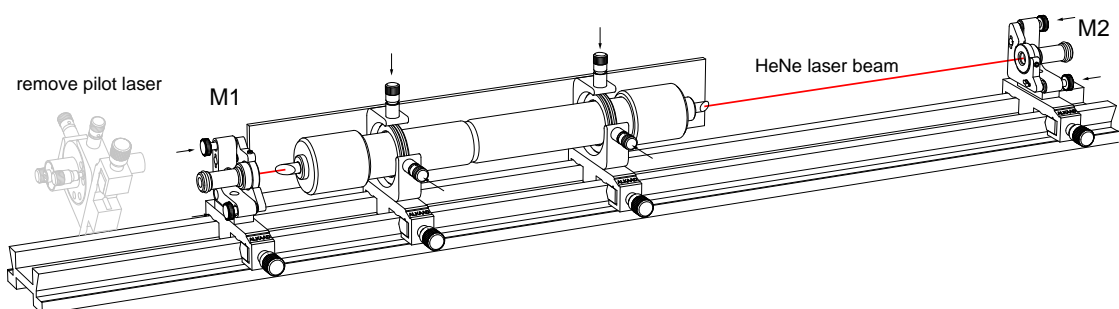
4.1.5 Start the laser

Figure 33: Placing the HeNe tube

Place the tube between both mirrors in such a way that the left side of the tube is close to the flat mirror. In the section of Gaussian beams we will learn why this is the best choice.

Switch on the discharge and the laser starts. Visually realign all adjustment screws for highest laser power.

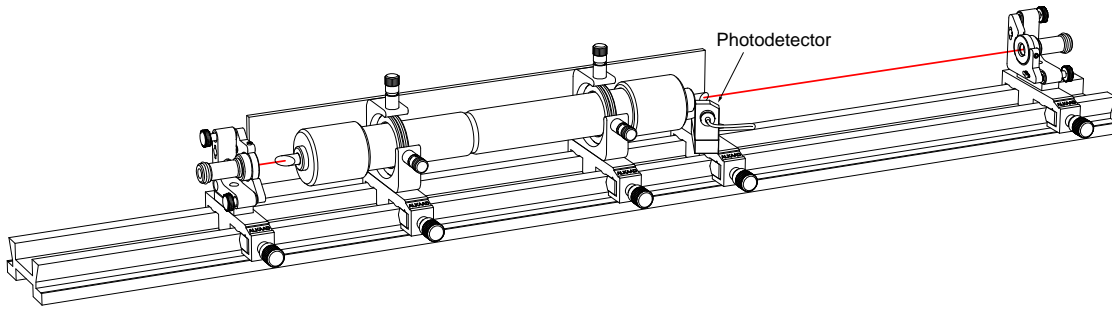### 4.1.6 Add the photodetector

Figure 34: Inserting the photodetector module

Now the photodetector is added. Make sure that the beam hits the sensitive area of the detector.

Maybe the tube must be slightly turned about its long axis in its holder to direct the reflex from the Brewster window to the centre of the detector.
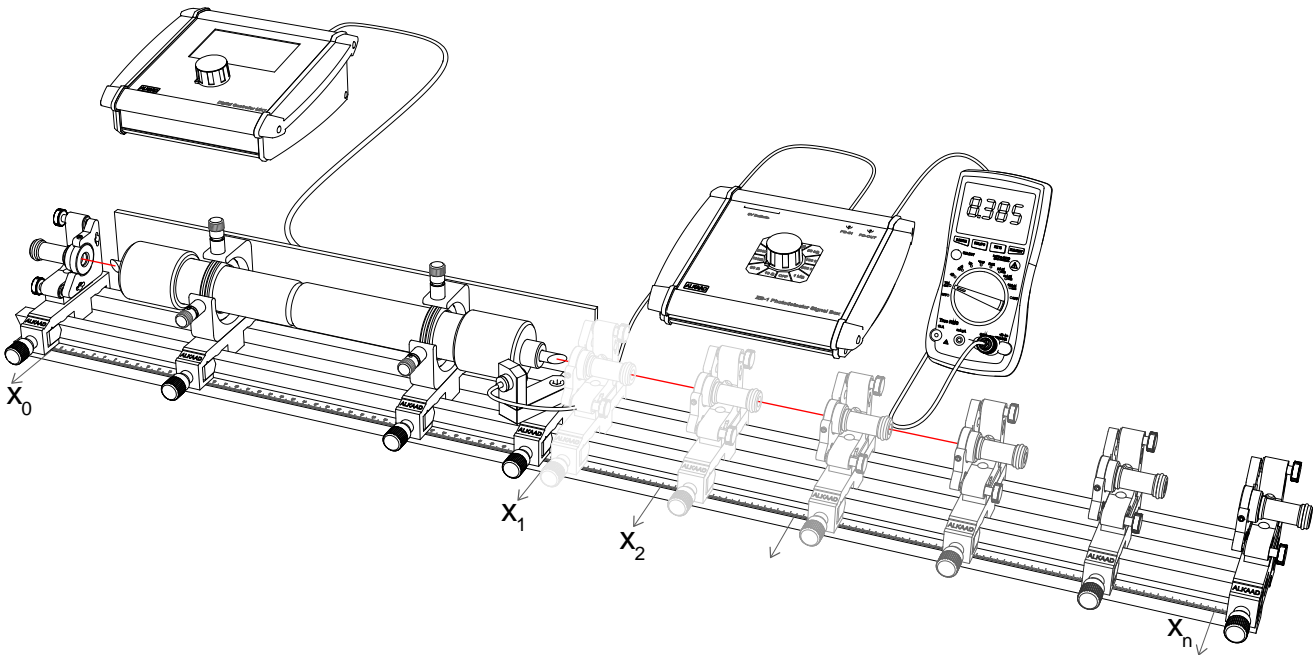
4.2 Optical stability criteria

Figure 35: Determination of the optical stability of the cavity

The stability criterion for optical cavities was introduced by Kogelnik and Li [13] and is derived as $0 \leq g_1 \cdot g_2 \leq 1$ whereby $g_i = 1 - L/R_i$.

L is the distance between the mirrors and R_i is the radius of curvature of mirror M_i.

In our set-up we are using a flat mirror on the left side and a curved one on the right side. In the first set-up we will use the mirror having a radius of curvature R of 750 mm. The stability criterion of resulting hemispherical cavity therefore is

$$0 \leq (1 - \frac{L}{R_{left}}) \cdot (1 - \frac{L}{R_{right}}) \leq 1 \text{ so here } 0 \leq (1 - \frac{L}{0.75m}) \leq 1$$

That means only for values of L in the range of 0...0.75 m the resonator can be stable. Calculating the same for 1 m of radius of curvature of the right mirror yields 1 m as maximum mirror distance.

To verify these findings we are measuring for both mirrors the output power versus the mirror distance L as shown in 36.
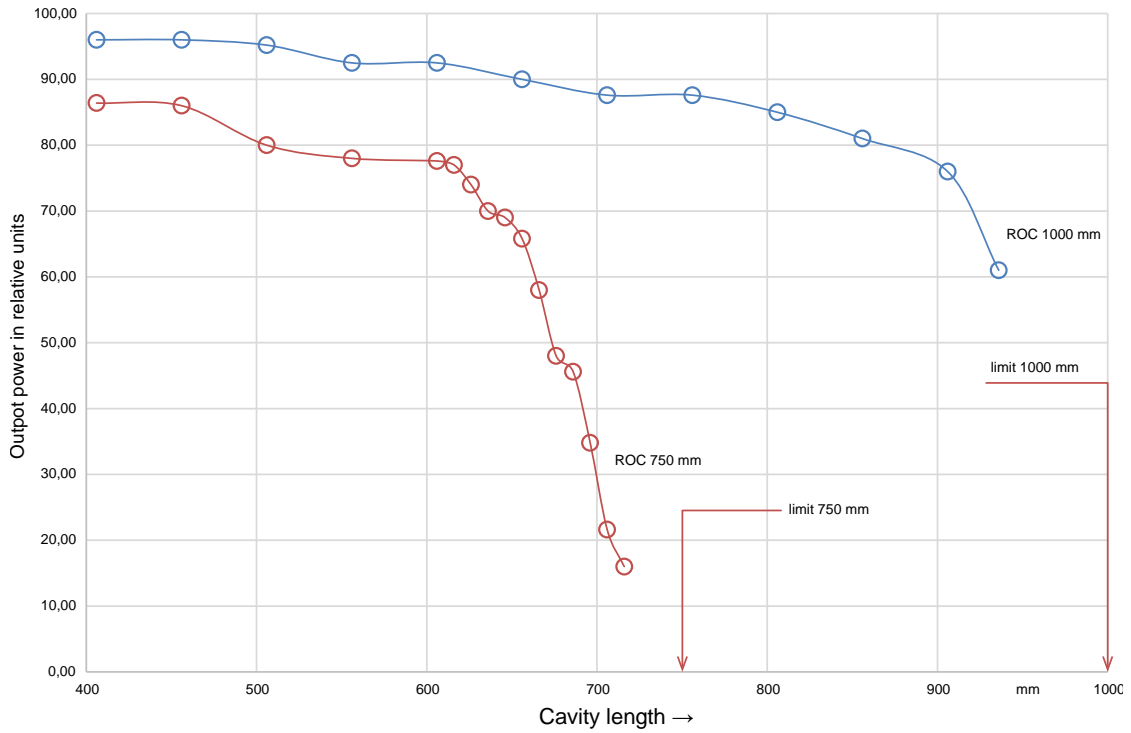
Figure 36: Verification of the stability criterion or radius of curvature (ROC) 750 and 1000 mm
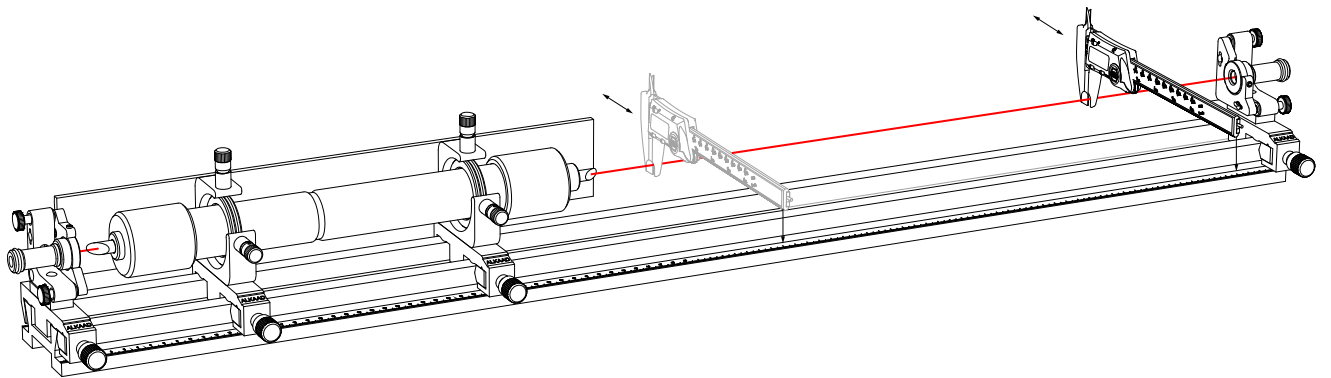
4.3   Gaussian beams

Figure 37: Measuring the beam diameter inside the cavity

Useful equations:

$$w_1^2 = \frac{L \cdot \lambda}{\pi} \cdot \sqrt{\frac{g_2}{g_1 \cdot (1 - g_1 \cdot g_2)}}$$

is the spot size at mirror M1. In our setup is $g_1 = 1$ and $g_2 = 1 - \frac{L}{R}$.

With $R = 1$ m, $g_2 = 1 - L$ results in: $w_1^2 = \frac{L \cdot \lambda}{\pi} \cdot \sqrt{\frac{1-L}{L}}$

$$w_2^2 = \frac{L \cdot \lambda}{\pi} \cdot \sqrt{\frac{g_1}{g_1 \cdot (1 - g_2 \cdot g_2)}}$$

is the spot size at mirror M2. $w_2^2 = \frac{L \cdot \lambda}{\pi} \cdot \sqrt{\frac{1}{(1-L) \cdot L}}$

$$w(z) = w_0 \cdot \sqrt{1 + (\frac{z}{z_R})^2}, \text{ with } z_R = \pi \cdot \frac{w_0^2}{\lambda}$$

with the beam waist width w_0 and the Rayleigh range z_R this equation yields the beam width $w(z)$ as function of the position z inside the cavity.

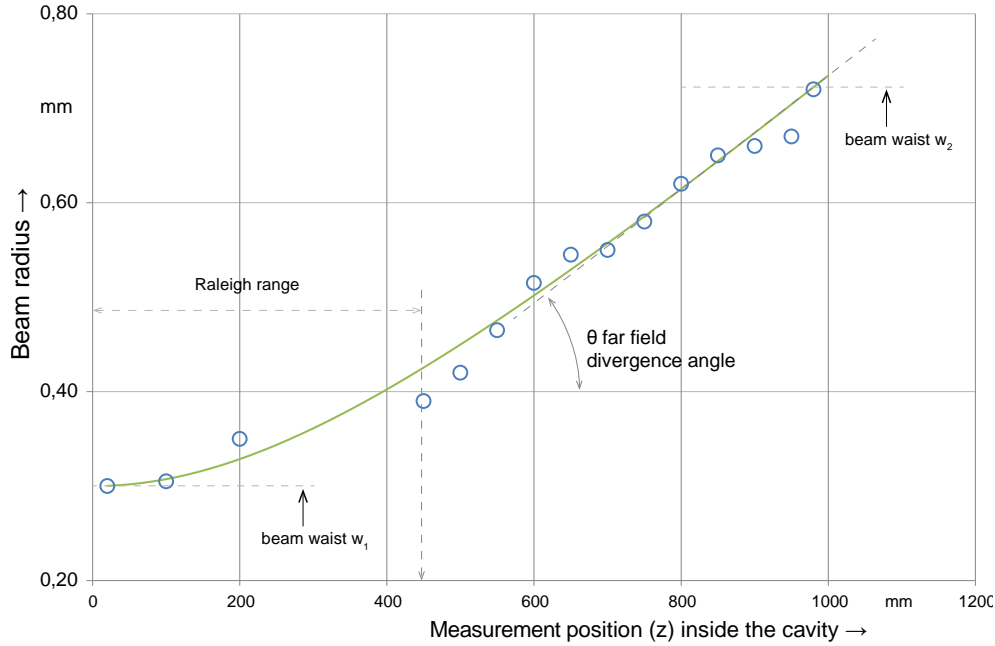$$\theta = \frac{2 \cdot \lambda}{\pi \cdot w_0}$$

is the far field angle

Figure 38: Measured beam diameter as function of the position inside the cavity relative to left mirror
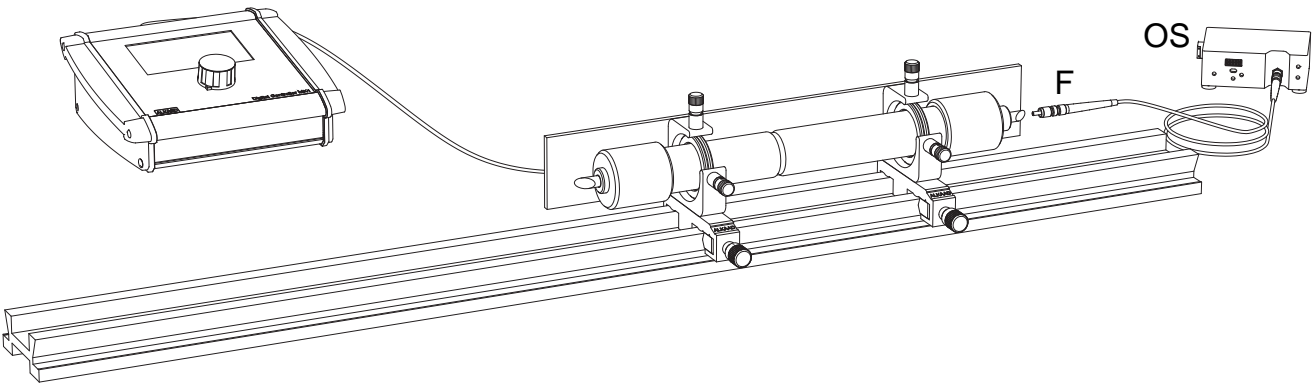
4.4   Excitation spectrum

Figure 39: Set-up to measure and record the excitation spectrum

We are using a spectrum analyser (OS) equipped with an optical fibre (F). The excitation fluorescence is strong enough that holding the fibre in direction of the Brewster window results in an almost noise free signal. A spectrum recorded that way is shown in 40.

The resolution of the spectrum analyser is just 2 nm and a better one will yield more resolved lines. However, with this simple spectrum analyser the fluorescence lines can be assigned to the transitions of the energy level diagram as shown in 5.

4.5   Wavelength selection and tuning

As mentioned in chapter 2, the Helium Neon laser has the potential to oscillate on different wavelengths. The goal of wavelength selection and tuning is to tune to as many as possible of these wavelengths.

In principle a laser oscillates on a wavelength for which the amplifier gain is highest and resonator losses are lowest.

The amplification gain is wavelength dependent and determined basically by the laser material. The losses, which determine the resonator quality, are also wavelength dependent and determined by the laser resonator cavity.

For each specific wavelength a set of mirrors could be created with an appropriate coating that is high reflective for this wavelength and otherwise transparent, but this is a quite cumbersome way to select a specific wavelength and such pairs of mirrors are expensive. It would be much better just to turn a knob to tune to a different wavelength.
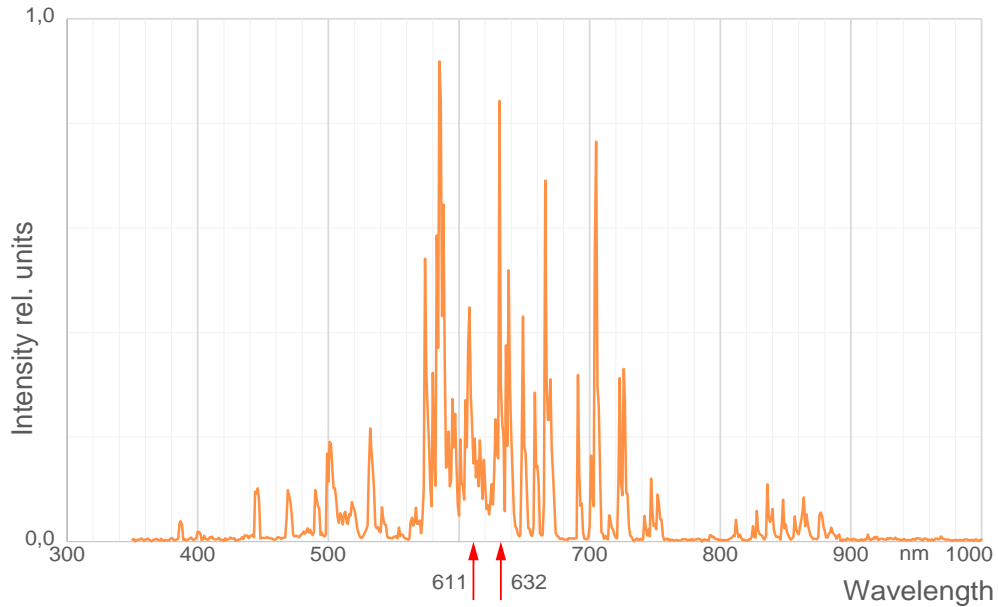
Figure 40: Helium Neon fluorescence spectrum in the range of 350...1000 nm

Such devices exist, one of them is the so called Littrow Prism, see figure 41 and another one is the birefringent tuner. In the set-up of Fig. 44 we are using a birefringent tuner which is placed into the cavity. To avoid larger insertion losses the birefringent or double refractive plate is turned to Brewster's angle.

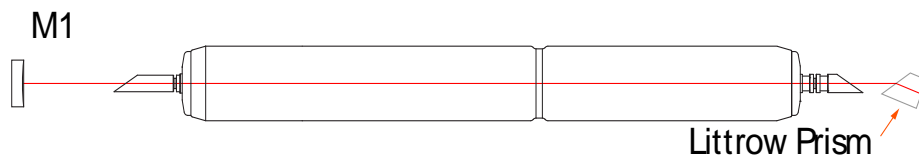### 4.5.1 Wavelength selection with Littrow prism

Figure 41: Principle of Littrow prism tuning

Using a Littrow prism for laser line tuning requires a modification of the laser cavity. Since the reflecting surface of the prism is flat, the flat mirror will be exchanged against the Littrow prism. Otherwise it would result in a cavity with two flat mirrors. Such a resonator cavity would be on the brim of optically stability and is for gas lasers with their low amplification not practical.
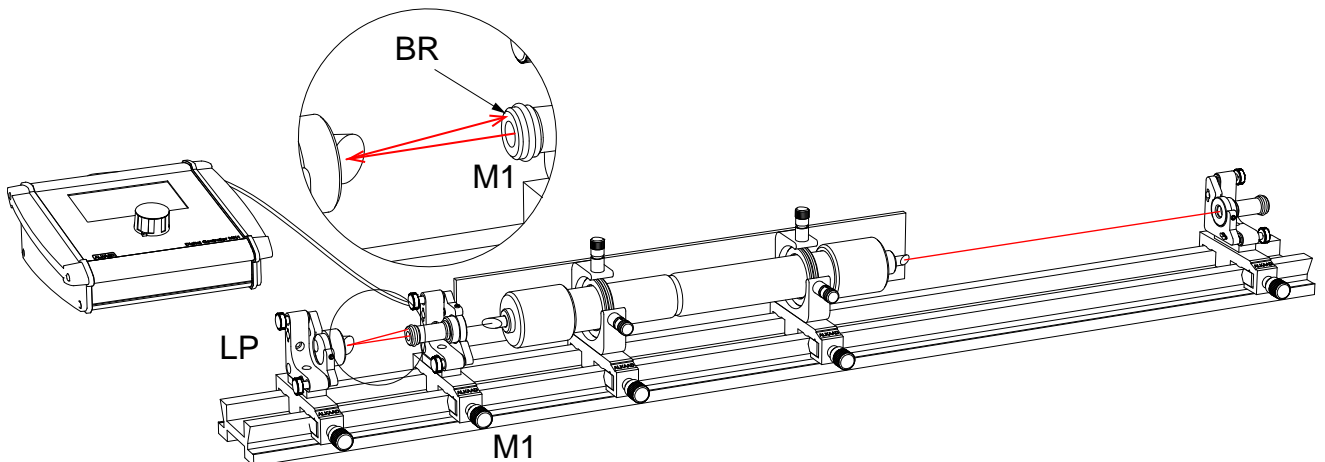

Figure 42: Aligning the Littrow prism tuner

It is good practise to align the Littrow prism (LP) with the laser beam which emerges from the left mirror M1.

Align the reflected light from the LP with the centre of the mirror mount. The closer the alignment is reached the more reflections appear. Best alignment is achieved, when the back reflecting beam starts to flicker which indicates a close-coupled cavity.

Remove the laser mirror M1. Now laser operation should occur with the Littrow prism as left cavity mirror. Align for maximum brightness. Move the Littrow prism close to the laser tube.

Once the entire system is optimised one can start to tune to other lines by turning the fine pitch screw (H) for the horizontal tilting.

Note: **It might be a good idea to clean the Brewster windows as well as the surface of the Littrow prism.** The orange line at 611 nm has a lower amplification gain compared to the 632.8 nm line, so losses due to dirt will prevent its oscillation first.
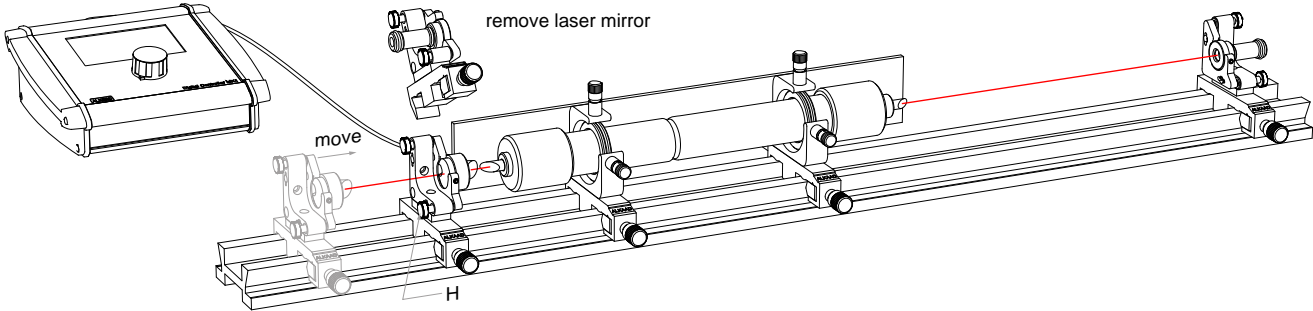

Figure 43: Removing the flat mirror M1
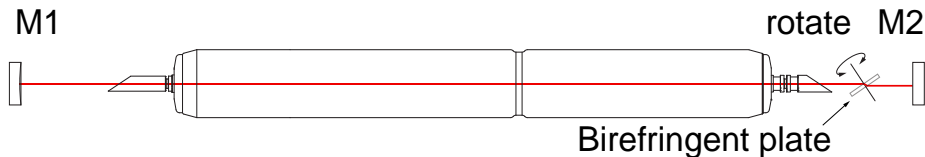
4.5.2   Wavelength selection with BFT

Figure 44: Principle of line tuning with a birefringent plate

The Brewster windows force the Helium Neon laser to operate on strictly linear polarised light. Inserted at an arbitrary angle, the birefringent plate changes the state of polarisation. So the light after passing the plate two times would partly be reflected out of the cavity at the Brewster windows. Those losses would stop the oscillation.

If the birefringent plate is rotated around its axis, the state of polarisation after the plate is varying because the polarisation depends on the difference δ in phase retardation between "ordinary" and "extraordinary" rays and the fraction of light belonging to either ray, generally producing some elliptic polarisation state. While the ordinary refractive index does not depend on the incident angle, the extraordinary does, so by turning the plate the phase difference changes.
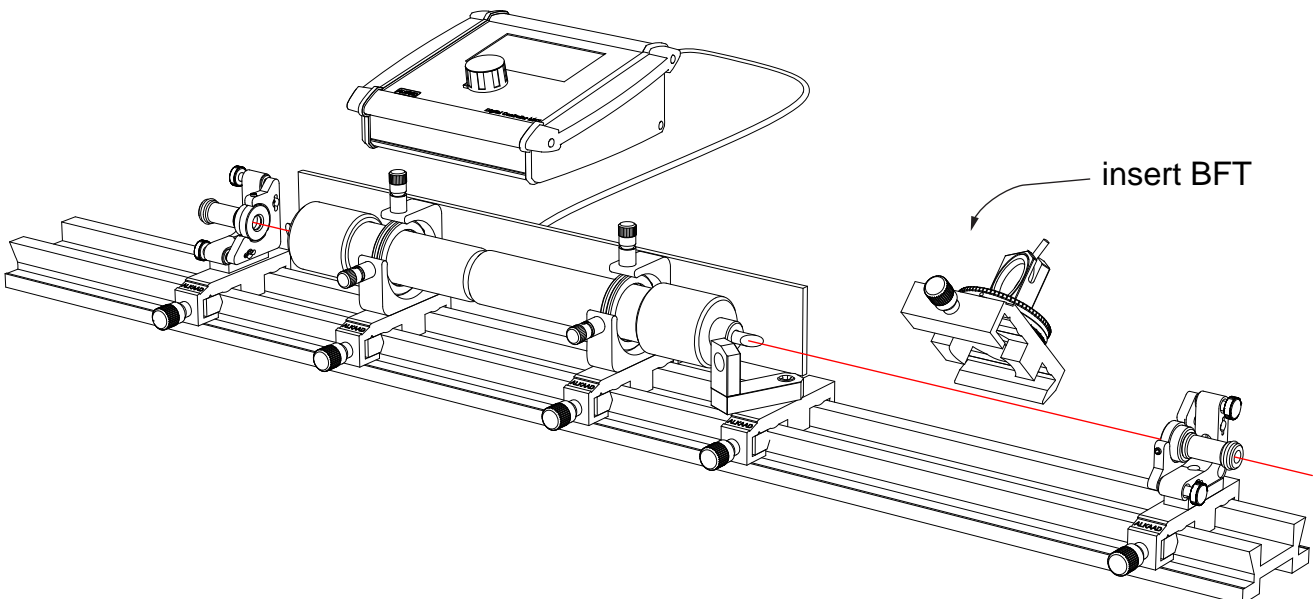

Figure 45: In a well optimised setup the birefringent tuner is inserted

If we set the plate to an angle where the phase shift between both rays is just $^\lambda/_2$, the returning beam is shifted again by $^\lambda/_2$ resulting in a total phase shift of λ between both rays which means the polarisation is not influenced and linear again and the laser can oscillate on that specific wavelength.
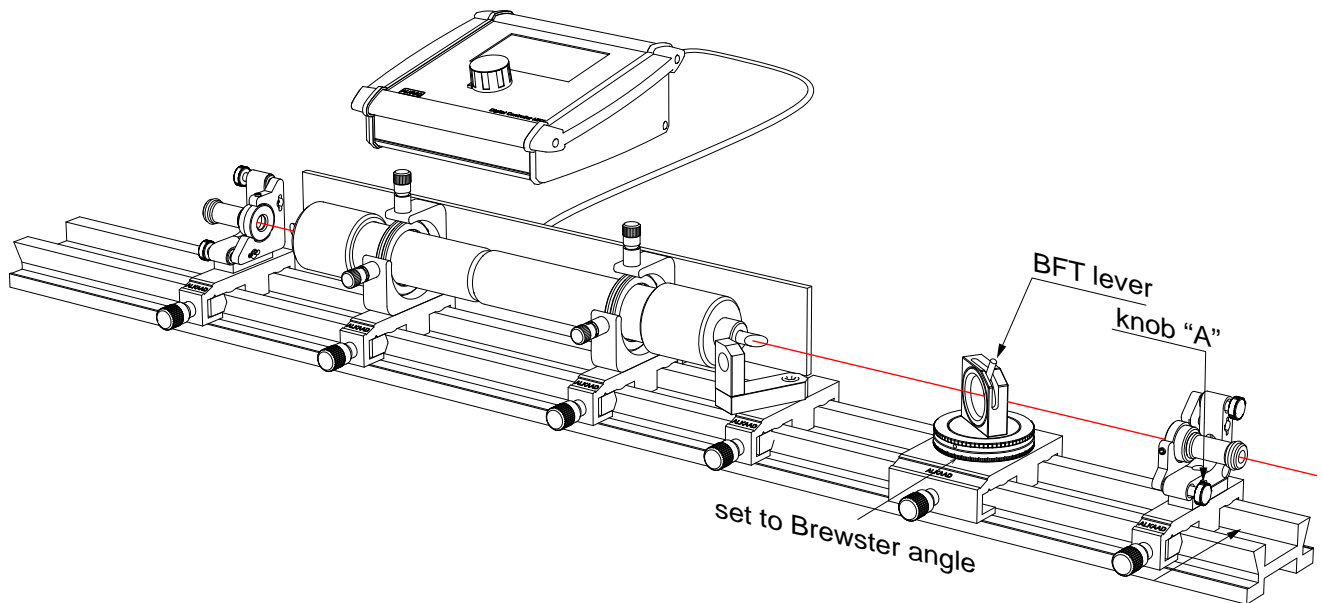

Figure 46: Bringing back the laser oscillation

Set the birefringent plate to the Brewster angle (57Â°). When rotating the birefringent plate by tilting the lever (L) laser emission should occur. If not, lift the lever up and down while adjusting the knob A to compensate the beam deviation caused by the quartz plate. Then gently tune to the maximum of performance and optimise the alignment of the mirror M2. By tilting the lever some other wavelength should show up.

If no light is branched to the extraordinary ray (lever (L) in vertical position), then there is no polarisation change and no wavelength selective filtering. In that condition the Brewster angle can be searched for by optimising the laser output turning the rotary plate (B), refer to figure 20.

Note: **It is very important that the Brewster window of the laser tube as well as the birefringent plate is cleaned and no dust particles are visible.**
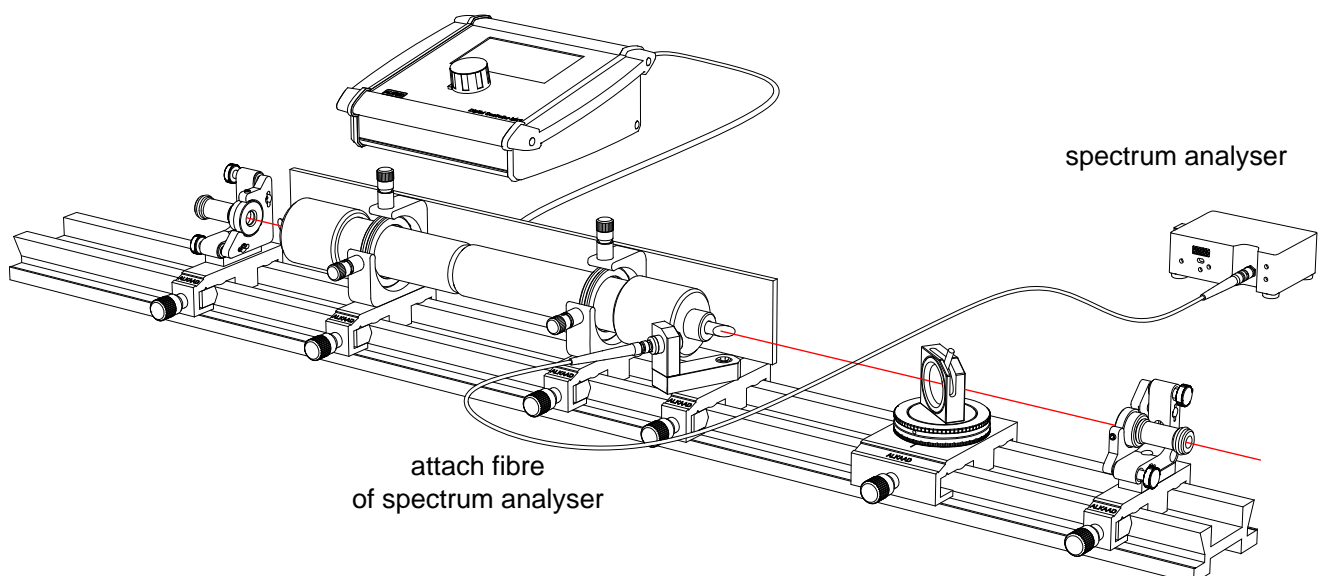

Figure 47: Connect the fibre of the spectrum analyser by using the 12 mm SMA fibre adapter
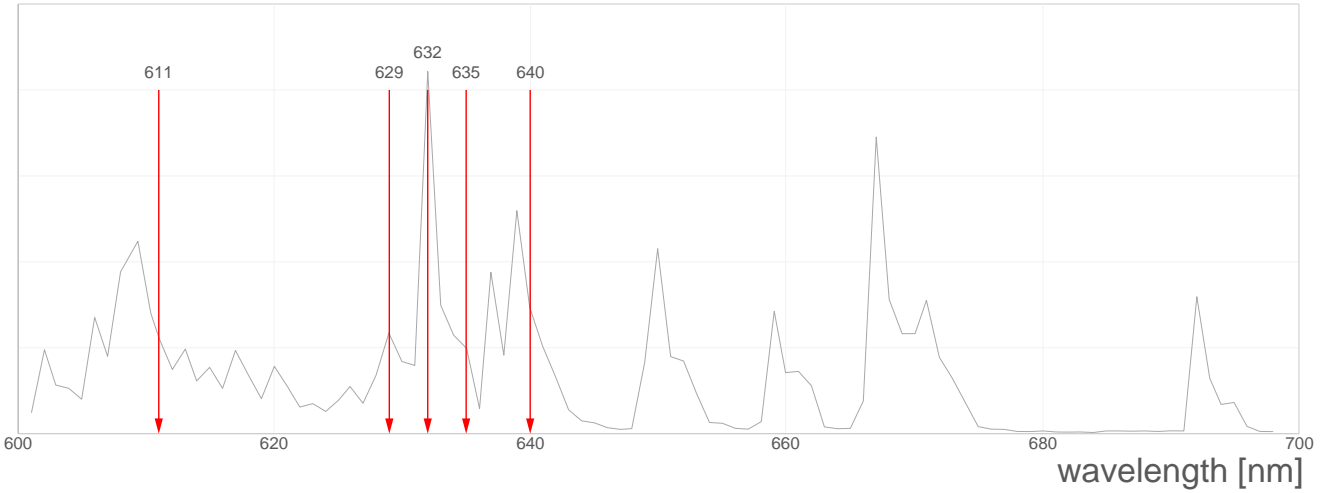
Figure 48: Observed lines drawn into the fluorescence spectrum

Five lines can be observed rotating the birefringent plate. It is recommended to make use of such an optical spectrum analyser since the colour of the lines does not change significantly, except the for orange line at 611 nm.

Wavelength	Strength
611.8 nm	10
629.8 nm	20
632.8 nm	100
635.2 nm	6
640.1 nm	34

Table 2: Observable lines and strength

4.6   HeNe laser modes

A free running laser will operate on all possible cavity modes as long as gain is provided. Due to the inhomogeneously broadened gain profile [11] the Helium Neon laser can oscillate on a number of modes which are defined by the losses and the length L of the cavity.
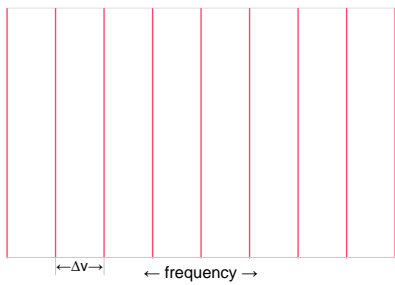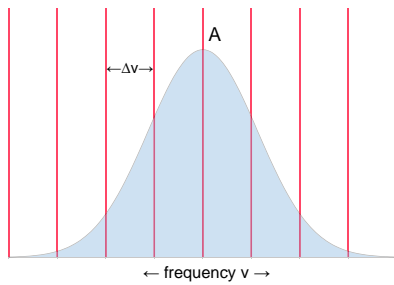

Figure 49: Empty cavity
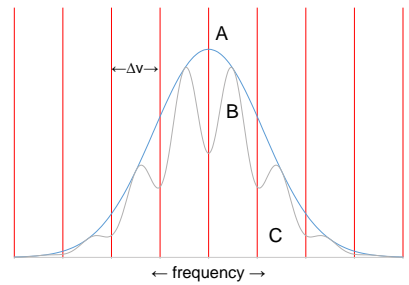

Figure 50: Cavity with amplifying Neon

Figure 51: Longitudinal multimode oscillation

An empty cavity with a mirror spacing of L can accommodate stable modes which fulfil the condition:

$$N \cdot \frac{\lambda}{2} = L$$

N is an integer and not small, for example N is 1.6 million for wavelength $\lambda = 632$ nm and the cavity length 1 m. The difference frequency $\delta\nu$ of two neighboured modes is consequently:

$$\delta\nu = \frac{c}{2 \cdot L}$$

Only for those stable modes the resonator quality is high, that is the losses are small.

If such a cavity is filled by amplifying Neon as shown in figure 50 a couple of modes are within the gain profile width (A). Laser oscillation occurs when the resonator losses are compensated by the amplifier gain.

Where the population of exited states feeding the laser oscillation gets depleted, so called hole burning of the gain profile (A) can result and the gain profile gets modified (B).

For a number of longitudinal modes, the oscillation condition can be fulfilled, that is the gain is sufficient for different frequencies to oscillate resulting in a laser beam which consists of different frequencies.

Some applications demand an extreme purity of the laser frequency and a high coherence length. So only one mode should oscillate.

This can be achieved by two means: First the length of the laser cavity L could be reduced so the distance of the modes $\delta\nu$ is increased in such a way that only one mode is within the gain profile. However this method also reduces the length of the amplifying medium resulting in low available laser power. Another method is the use of a so called etalon.
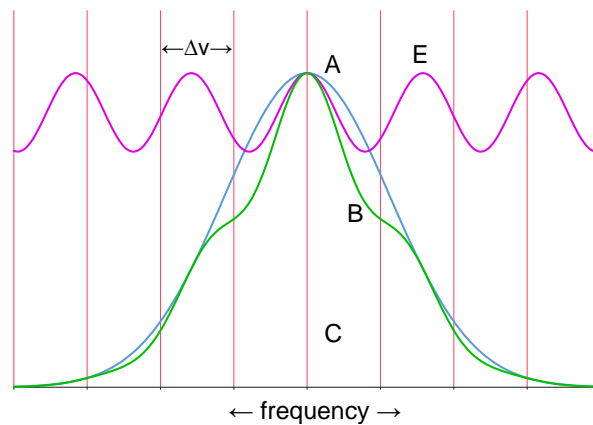
4.6.1   Single mode operation with etalon

Figure 52: The transmission profile of the etalon (E) folded with the gain curve (A) resulting in modified gain profile (B)

Inserted into the cavity the etalon introduces periodic extra losses because of reflection at its surfaces. The surface reflexes only interfere constructively for integer multiples of wavelengths inside the etalon. So the etalon with its transmission profile modulates the net gain profile to curve (B) of figure 52. By selecting a suitable length of the etalon, single mode operation can be achieved.

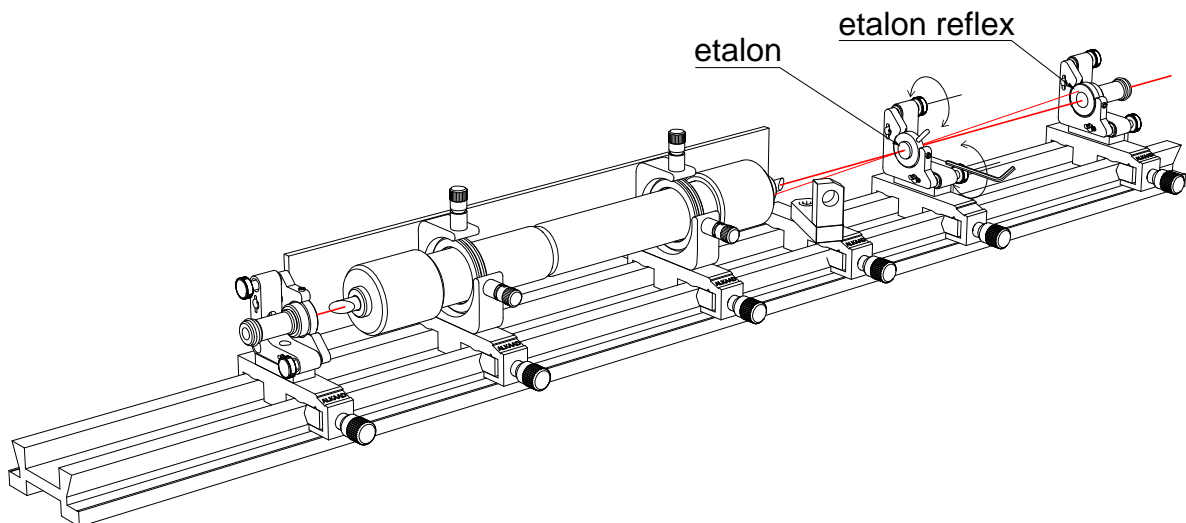In our experiment the length of the etalon is 1 cm.

Figure 53: The etalon is placed onto the rail into an optimised setup.

In a well optimised laser the etalon is placed as shown in figure 53. Align the etalon by turning the adjustment knobs to achieve laser oscillation. Observe the reflex which is created by the etalon in case it is not exactly aligned perpendicular to the beam.

Align the etalon in such a way that it is aligned perpendicular to the beam. By turning either the knob for horizontal or vertical tilt in one direction, different orders of the etalon are observed. That means that the laser oscillation ceases and comes back when continuing tilting.

4.6.2 Longitudinal modes

From the preceding chapter we already know that the experimental Helium Neon laser will operate on different longitudinal modes simultaneously. We also notice that the difference or beat frequency of two neighboured mode depends on the cavity length L (the spacing between the mirror). For a length of 1 m of the cavity we calculate a beat frequency of 150 MHz.

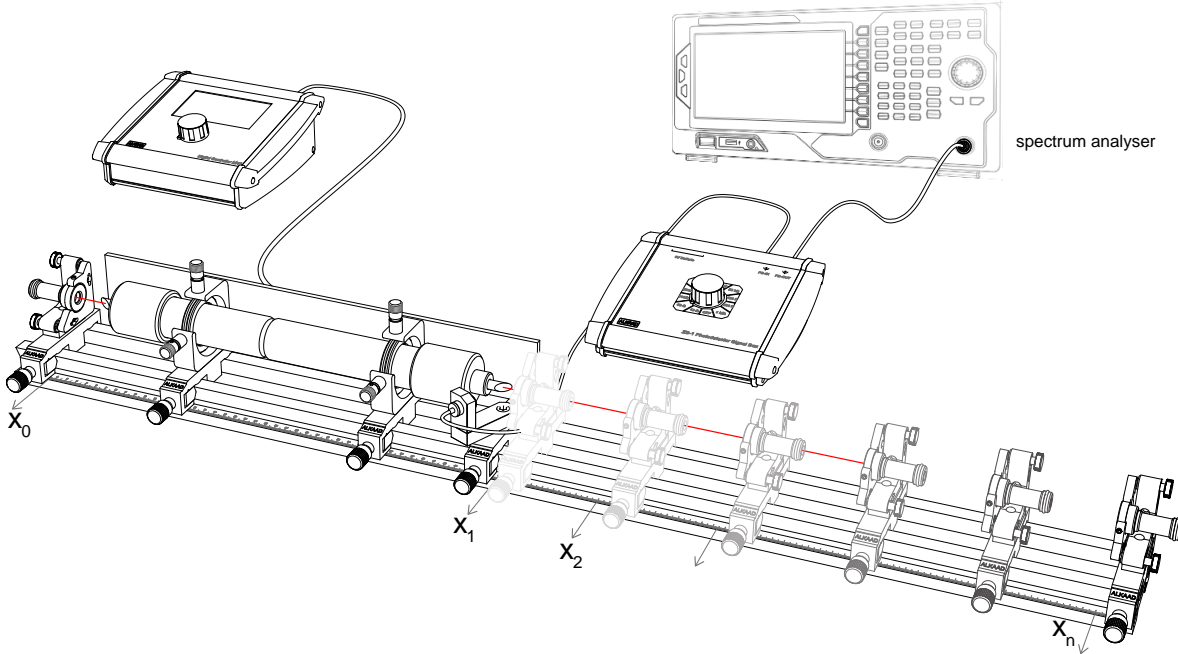$$\delta\nu = \frac{c}{2 \cdot L} = \frac{3 \cdot 10^8 \text{m/s}}{2 \cdot 1m} = 150 \text{MHz}$$

Figure 54: Measuring the beat frequency of longitudinal modes with an electronic spectrum analyser

The provided photodetector as well as the signal conditioning box are able to detect such fast optical signals. The ZB1 box is switched to a shunt of 50 Ohms and connected to the spectrum analyser.
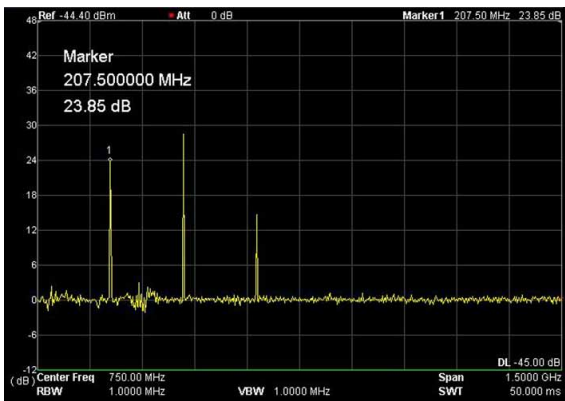

Figure 55: Monitor display of a measurement, showing beside the peak of $\delta\nu$ some other harmonics
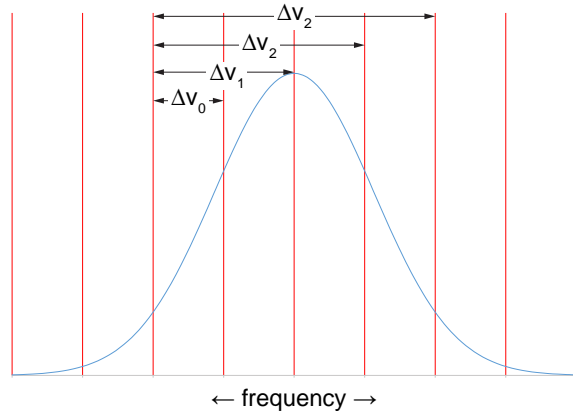

Figure 56: Simultaneously oscillating modes creation a progression of beat frequencies

Beside the peak related to $\delta\nu$ the spectrum analyser surprisingly shows some more peaks. Recalling that the laser oscillates on a couple of modes, there will be also beat frequency contributions from the over next neighbouring mode and so on.

Depending on the number of oscillating longitudinal modes we will notice a progression of peaks. Five modes are oscillating in the example of Fig. 55 creating four beat frequencies. The number of beat frequencies tells how many modes oscillate in the laser.

By using this novel method we can study the longitudinal modes in detail by measuring their beat frequencies with high accuracy. We can impressively verify the dependence of the beat frequency on the cavity length and can detect how many modes are oscillating. This is fascinating.
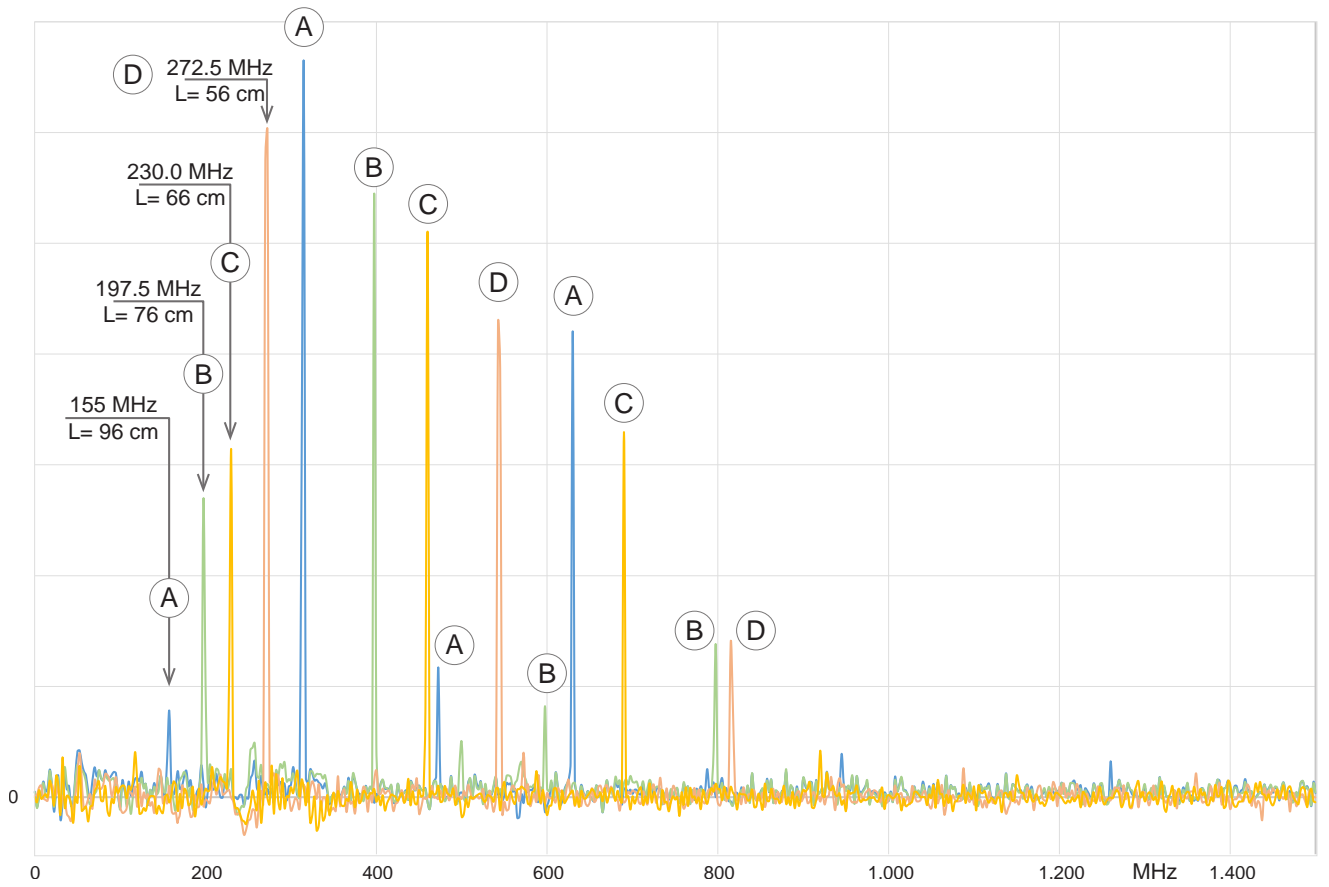
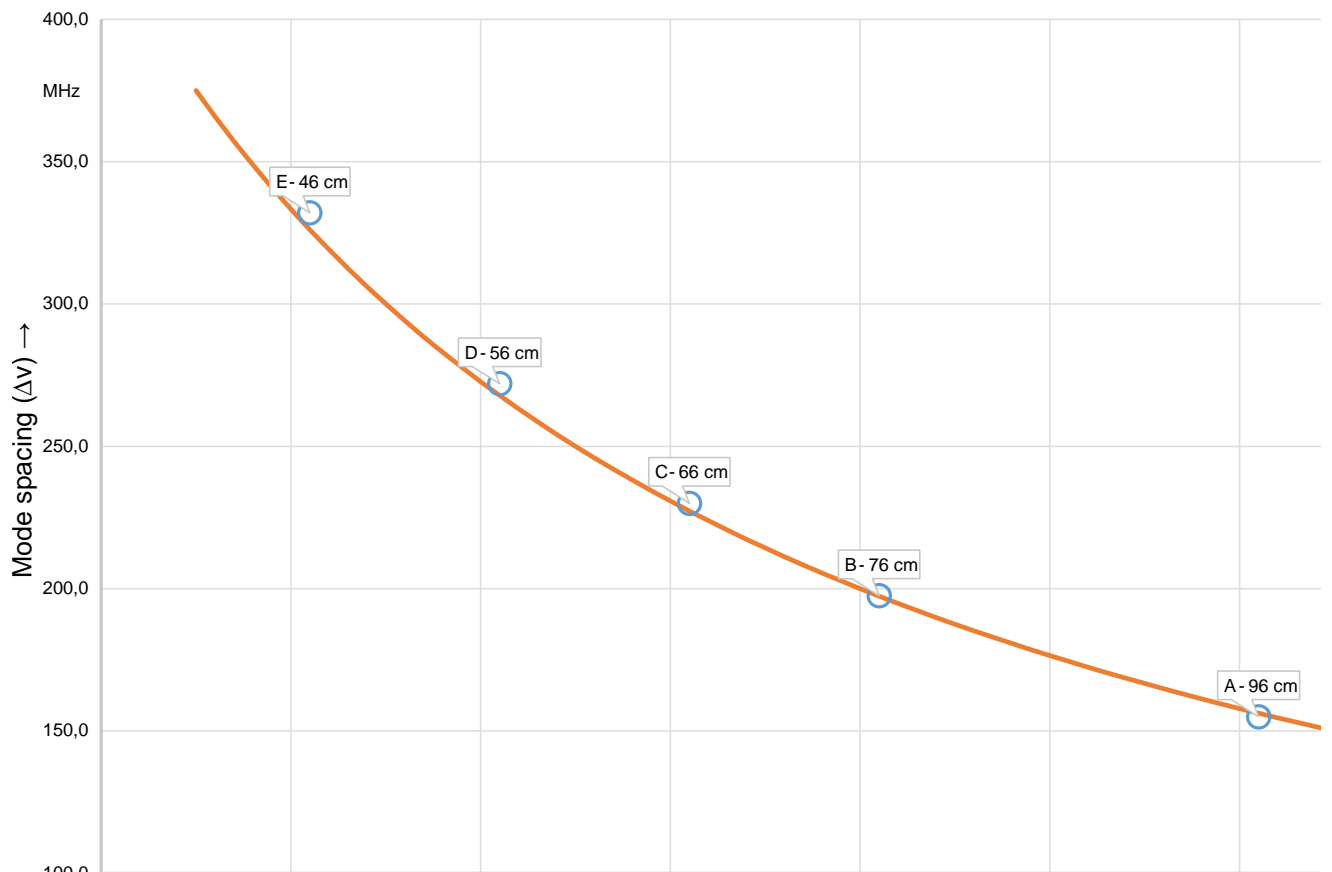Figure 57: Tracks of the spectrum analyser for a cavity length of 96 cm (A), 76 cm (B), 66 cm (C) and 56 cm(D)

Figure 58: Measurement of the mode beat frequency versus cavity length

References

[1] T. H. Maiman. Stimulated optical radiation in ruby. *Nature*, 187(4736):493–494, 1960.

[2] A. Javan. The history of the laser. http://alijavan.mit.edu/.

[3] D. R. Herriott A. Javan, W. R. Bennett. Population inversion and continuous optical maser oscillation in a gas discharge containing a he-ne mixture. *Physical Review Letters*, 6(3):106–110, 1961.

[4] A.D. White and J.D. Rigden. Continuous gas maser operation in the visible. *Proc. IRE*, 50(1):1697, 1962.

[5] A. L. Schawlow and C. H. Townes. Infrared and optical masers. *Phys. Rev.*, 112(8):1940, 1958.

[6] L. G. Van Uitert J. E. Geusic, H. M. Marcos. Laser oscillations in nd-doped yttrium aluminum, yttrium gallium and gadolinium garnets. *Appl. Phys. Lett.*, 4(10):182, 1964.

[7] A. E. Siegman. *Lasers*. University Science Books, 1986.

[8] W. Luhs. Diode pumped nd:yag laser. http://repairfaq.ece.drexel.edu/sam/MEOS/EXP0578.pdf, 1992. MEOS GmbH.

[9] Platinum-iridium meter bar. http://en.wikipedia.org/wiki/Metre.

[10] B. Struve W. Luhs and G. Litfin. Tunable multiline he-ne laser. *Laser Optoelectronics*, 1986(18):319–357, 1986.

[11] W. Luhs. Experiment 06 helium neon laser. http://repairfaq.ece.drexel.edu/sam/MEOS/EXP06.pdf, 1999. MEOS GmbH.

[12] Safety of laser products part 1: Equipment classification, requirements and user's guide. http://www.ee.washington.edu/people/faculty/darling/ee436s14/IEC_60825_1.pdf, 2001.

[13] H. Kogelnik and T. Li. Laser beams and resonators. *Applied Optics*, 5(10):1550–1567, 1966.